Synchronization of Multiple Chaotic Gyroscopes Using the Fundamental Equation of Mechanics

Firdaus E. Udwadia
Professor
Departments of Mechanical and Aerospace Engineering, Civil Engineering, Mathematics, Systems Architecture Engineering, and Information and Operations Management,
University of Southern California,
430K Olin Hall,
Los Angeles, CA 90089-1453
e-mail: fudwadia@usc.edu

Byungrin Han
Graduate Student
Department of Mechanical and Aerospace Engineering,
University of Southern California,
Los Angeles, CA 90089-1453

This paper provides a simple, novel approach for synchronizing the motions of multiple "slave" nonlinear mechanical systems by actively controlling them so that they follow the motion of an independent "master" mechanical system. The multiple slave systems need not be identical to one another. The method is inspired by recent results in analytical dynamics, and it leads to the determination of the set of control forces to create such synchronization between highly nonlinear dynamical systems. No linearizations or approximations are involved, and the exact control forces needed to synchronize the nonlinear systems are obtained in closed form. The method is applied to the synchronization of multiple, yet different, chaotic gyroscopes that are required to replicate the motion of a master gyro, which may have a chaotic or a regular motion. The efficacy of the method and its simplicity in synchronizing these mechanical systems are illustrated by two numerical examples, the first dealing with a system of three different gyros, the second with five different ones. [DOI: 10.1115/1.2793132]

1 Introduction

Gyrodynamics is an area of mechanics that has been of significant interest for more than a century to both the scientific and the engineering communities. Gyroscopes, from a purely scientific viewpoint, show many strange and interesting properties, and from an engineering viewpoint, they have great utility in the navigation of aircraft, rockets, and spacecraft and in the control of complex mechanical systems. It has been known for some time now [1–6] that symmetric gyros, when subjected to harmonic vertical base excitations, exhibit a variety of interesting dynamic behaviors that can span the range all the way from regular to chaotic motions. Various investigators have looked at gyro models that involve different types of damping, the most common type being linear plus cubic [3–5]. Depending on the parameters that describe these gyrosystems, they can exhibit fixed points, periodic behavior, period doubling behavior, quasiperiodic behavior, and chaotic motions.

Synchronization of two chaotic systems is an important problem in nonlinear science, and it has received considerable attention in recent years since it was first carried out by Pecora and Carroll [7] and Lakshmanan and Murali [8]. When one has more than one gyro operating in a mechanical system, synchronizing these gyros so that a master gyro drives a bunch of slave gyros in such a manner that the slaves "exactly" replicate the motion of the master is a problem of considerable interest both in navigation and in the transmission of encrypted messages [9]. While many researchers have considered the synchronization of two coupled chaotic systems whose motions may or may not synchronize depending on the coupling between them, in this paper we consider the synchronization of a set of "slave" mechanical systems that may or may not be coupled, each synchronized to the motions of an independent "master" mechanical system.

The way the synchronization of the motion of two chaotic systems has been usually achieved—the systems are usually, it appears, taken to be *identical*, but starting with different initial conditions—is through the application of a control signal (a coupling) to one of them (the slave system), which is often some linear or nonlinear function of the difference in the motion between the master and the slave. The methodology is perhaps best described as belonging to a kind of generalized feedback control philosophy. For example, Chen [4] considered two identical chaotic gyros, used a variety of such control laws, and showed that when the feedback gain exceeds a certain value, the slave gyro synchronizes with the master gyro. The value of this feedback gain, above which such synchronization occurs, is typically obtained through numerical experimentation [4]. Modern nonlinear control theory has also been used to look at the gyro synchronization problem. Here, the system is conceived as an autonomous set of first order nonlinear differential equations, and the difference in the response between the master and the slave gyro is taken to be an error signal. A suitable time-varying control is then applied to the slave gyro to drive this error signal to zero. Often, this is done by using feedback linearization; the nonlinear terms in the equation governing the error signal are eliminated, and then standard linear feedback control theory is applied [10]. Such strategies, which may be commonly found in the literature, become difficult, if not impossible, to use when we have many slaves that may be coupled to one another (not just one) and that need to be driven to yield the same motions as a single independent master, and especially so when the dynamical characteristics of these slaves are *not* identical with one another and/or with those of the master gyro. Considering that it is very difficult to exactly replicate the properties of multiple mechanical systems even when they "seem" identical, it is interesting that the problem of driving *nonidentical* slaves using a master that may also be different from each of the slaves has only recently begun to be broached in the nonlinear science literature [11,12].

In this paper, we explore a new and different strategy for synchronizing the response of n nonlinear mechanical systems that is inspired by some recent advances in analytical dynamics [13]. We consider a system of n gyros—not necessarily identical—some, or all, of which may exhibit a chaotic behavior, and we pose the problem of synchronizing the motion of all the others with, say, that of the ith gyro (the master). We frame this in the context of a tracking control problem, in which the $n-1$ slave gyros are re-

Contributed by the Applied Mechanics Division of ASME for publication in the JOURNAL OF APPLIED MECHANICS. Manuscript received July 13, 2006; final manuscript received July 4, 2007; published online February 25, 2008. Review conducted by Oliver M. O'Reilly.

quired to exactly track the motion of the master gyro. We then further reformulate the tracking problem as a problem of constrained motion, where we want the control (constraint) forces to be such that all the gyros, which are highly nonlinear systems, are constrained to have the same motion. We use the explicit closed form analytical control given by the fundamental equation [13] to then yield the control force that will cause, in a theoretical sense, *exact* synchronization of these gyros. We show that this approach to the synchronization of such gyroscopic systems—and, indeed, general nonidentical, nonlinear mechanical systems—which is based on these deeper results from analytical mechanics, has several advantages, most important of which are that the control forces obtained are continuous functions of time and that they can be found in closed form and hence can be determined simply and efficaciously. Furthermore, in a sense, the minimum forces that need to be exerted to synchronize these nonlinear systems are obtained, and they yield, theoretically speaking, exact synchronization. As we shall show, of some importance is the fact that the manner in which synchronization is achieved can be controlled easily and with little difficulty.

The paper is organized as follows. In Sec. 2, we provide a brief description of the equation of motion of a symmetric gyro subjected to a vertical periodic base motion. We use the Lagrangian approach and obtain the requisite equations of motion. In Sec. 3, we present the fundamental equation that provides the explicit equation of motion for general nonlinear mechanical systems that are constrained. In Sec. 4 (and in Appendix B), we apply the fundamental equation to the problem of synchronizing n gyros, providing a closed form solution to the determination of the control forces required to be applied to each of these nonlinear systems that yields exact synchronization of their motions. In Sec. 5, we present several numerical results to illustrate the behavior of the proposed control, and its simplicity and efficacy. In the last section, we present our conclusions.

2 Equation of Motion for the Symmetric Gyro

Consider the symmetric gyro, whose point of support, o, undergoes a vertical harmonic motion of frequency ω and amplitude d_0, as shown in Fig. 1. Using the Euler angles θ (nutation), φ (precession), and ψ (spin) [14], the Lagrangian for the system is given by (see Appendix A[1])

$$L = \frac{1}{2}I(\dot{\theta}^2 + \dot{\varphi}^2 \sin^2\theta) + \frac{1}{2}I_3(\dot{\psi} + \dot{\varphi}\cos\theta)^2 - mr\dot{d}\dot{\theta}\sin\theta - mgr\cos\theta \tag{1}$$

where m is the mass of the gyro, $I := I_1 + mr^2$, $I_1 = I_2$ is the principal equatorial moment of inertia through the center of mass (c.m.) of the gyro, and I_3 is the polar moment of inertia about the symmetry axis. In Fig. 1, the point of support of the gyro is denoted by o, so that the moments of inertia about the axes ox and oy are each equal to I. The dots in Eq. (1) refer to differentiation with respect to time t. The quantity r denotes the distance along the polar axis of the c.m. of the gyro from its point of support, and $d(t) = d_0 \sin\omega t$ is the time-varying amplitude of the vertical support motion that has frequency ω.

Since φ and ψ are cyclic coordinates, the corresponding angular momenta $p_\psi = I_3(\dot{\psi} + \dot{\varphi}\cos\theta)$ and $p_\varphi = I\dot{\varphi}\sin^2\theta + p_\psi\cos\theta$ are conserved. The angular velocities $\dot{\varphi}$ and $\dot{\psi}$ can be eliminated by using the Routhian [14],

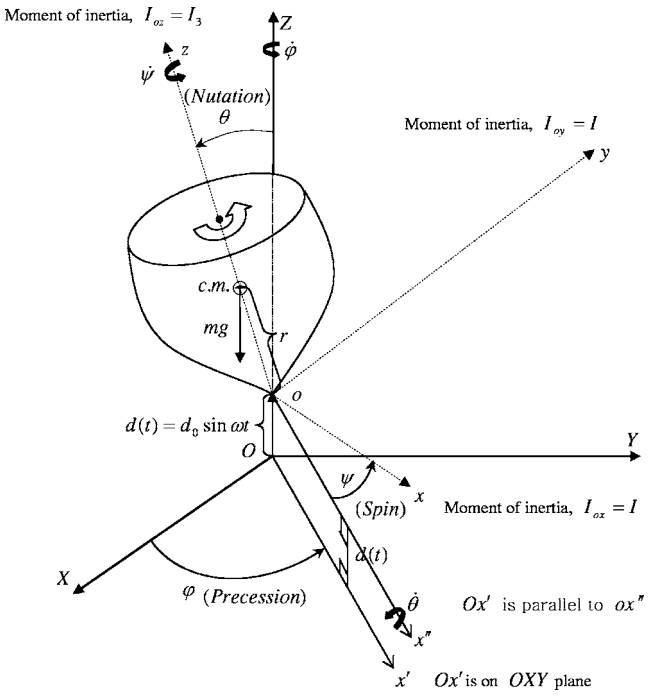

Fig. 1 Symmetric gyroscope with vertical support excitation $d(t) = d_0 \sin(\omega t)$

$$R(\theta, \dot{\theta}, t) = L - p_\varphi\dot{\varphi}(p_\varphi, p_\psi, \theta) - p_\psi\dot{\psi}(p_\varphi, p_\psi, \theta) \tag{2}$$

The equation of motion, which is given by $(d/dt)(\partial R/\partial\dot{\theta}) - \partial R/\partial\theta = F_d$, then reduces to

$$I\ddot{\theta} + \frac{(p_\varphi - p_\psi\cos\theta)(p_\psi - p_\varphi\cos\theta)}{I\sin^3\theta} - mgr\sin\theta - mr\sin\theta\ddot{d}(t) = F_d \tag{3}$$

where F_d is the nonconservative force of damping, which we take here to be of linear-plus-cubic type [3], so that $F_d = -\hat{c}\dot{\theta} - \hat{e}\dot{\theta}^3$. Along with previous researchers [2–5], for simplicity, we only consider damping related to the θ coordinate.

Were we to further assume that $p_\varphi = p_\psi = \bar{p}$ (which permits the gyro to be in the so-called "sleeping" position, removing the singularity in Eq. (2)), Eq. (3) can be further simplified to

$$\ddot{\theta} + \alpha^2\frac{(1-\cos\theta)^2}{\sin^3\theta} + c\dot{\theta} + e\dot{\theta}^3 - \beta\sin\theta = -\gamma\sin\theta\sin\omega t \tag{4}$$

Under this assumption, Eq. (4) then is the differential equation that describes the motion of the symmetric gyro, where we have denoted $\alpha = \bar{p}/I$, $c = \hat{c}/I$, $e = \hat{e}/I$, $\beta = mgr/I$, and $\gamma = \omega^2 mrd_0/I$. The parameter set $P = \{\alpha, \beta, c, e, \gamma, \omega\}$ specifies the physical characteristics of the gyro and the harmonic vertical motion of the base on which it is supported. It may be pointed out that no assumption on the magnitude of the vertical displacement d_0 of the base has been made in arriving at this equation. We note in passing that no singularity arises in Eq. (4) due to the $\sin\theta$ term in the denominator in Eq. (4).

3 Fundamental Equation

This equation deals with the explicit equation of motion for a mechanical system when the system is constrained to satisfy a set of consistent constraints. Consider an unconstrained discrete mechanical system whose equation of motion is described by the equations

[1]We provide the Lagrangian in Appendix A. This is specifically because the Lagrangian given in Ref. [2] is incorrect and, consequently, the equation of motion obtained from it is also invalid. Unfortunately, this error has found its way into the current literature dealing with this topic, as in Refs. [1–5] and Ref. [10].

$$\mathbf{M}(t,\mathbf{q})\ddot{\mathbf{q}} = f(\mathbf{q},\dot{\mathbf{q}},t) \quad \mathbf{q}(0) = \mathbf{q}_0 \quad \dot{\mathbf{q}}(0) = \dot{\mathbf{q}}_0 \tag{5}$$

where $\mathbf{M}$ is an $n \times n$ symmetric, positive definite matrix, the n vector $\mathbf{q}$ represents the generalized coordinates used to describe the configuration of the system, and the right hand side is a known function of $\mathbf{q}$, $\dot{\mathbf{q}}$, and t. The dots refer to differentiation with respect to time. By unconstrained we mean here that the components of the initial velocity $\dot{\mathbf{q}}_0$ can be arbitrarily specified. Equation (5) results from the application of Lagrange's equations to a mechanical system, or from Newtonian mechanics.

Let this system be subjected to a set of s constraints of the form

$$\mathbf{h}(\mathbf{q}(t)) = 0 \tag{6}$$

that are satisfied by the initial conditions so that

$$\mathbf{h}(\mathbf{q}_0) = 0 \quad \text{and } \dot{\mathbf{h}}(\mathbf{q}_0,\dot{\mathbf{q}}_0) = 0 \tag{7}$$

Here, $\mathbf{h}$, is an s vector. Differentiating Eq. (6) twice with respect to time, we obtain the set of matrix equations

$$\mathbf{A}(\mathbf{q},\dot{\mathbf{q}})\ddot{\mathbf{q}} = \mathbf{b}(\mathbf{q},\dot{\mathbf{q}}) \tag{8}$$

where $\mathbf{A}$ is an $s \times n$ matrix. The equation of motion of the constrained system that satisfies these constraints exactly is then explicitly given by [13]

$$\mathbf{M}\ddot{\mathbf{q}} = \mathbf{f}(\mathbf{q},\dot{\mathbf{q}},t) + \mathbf{F}^c(\mathbf{q},\dot{\mathbf{q}},t) \tag{9}$$

where

$$\mathbf{F}^c(\mathbf{q},\dot{\mathbf{q}},t) = \mathbf{M}^{1/2}(\mathbf{A}\mathbf{M}^{-1/2})^+(b - \mathbf{A}\mathbf{M}^{-1}\mathbf{f}) \tag{10}$$

Here, $\mathbf{X}^+$ denotes the Moore–Penrose (MP) inverse of the matrix $\mathbf{X}$ (see Ref. 13). We shall denote the n components of the n vector $\mathbf{F}^c$ by f_i^c, $i=1,2,\ldots,n$. We notice that the constraint (Eq. (6)) is actually implemented as Eq. (8). In what follows, we shall suppress the arguments of the various quantities unless needed for clarity.

When relations (7) are not satisfied by the initial conditions, one could replace the equation set (Eq. (8)) by any other system of constraint equations [15] whose solution asymptotically tends to $\mathbf{h}=0$, as $t \to \infty$. For example, the system of equations

$$\ddot{\mathbf{h}} + \mathbf{\Delta}\dot{\mathbf{h}} + \mathbf{\Sigma}\mathbf{h} = 0 \tag{11}$$

where $\mathbf{\Delta}$ and $\mathbf{\Sigma}$ are diagonal matrices with positive entries, would lead to $\mathbf{h} \to 0$ exponentially, as $t \to \infty$, and could be used by placing it in the form given in Eq. (8). It should be pointed out that the force $\mathbf{F}^c$ given by Eq. (10) minimizes, at each instant of time, the quantity $(\mathbf{F}^c)^T\mathbf{M}^{-1}\mathbf{F}^c$—the weighted norm of the active control force $\mathbf{F}^c$ [13].

The general results obtained in analytical mechanics (see Ref. [13] for more details) are far more extensive than those presented above; here, we have particularized them to only cover the present problem of interest—synchronization of n nonidentical gyroscopes (see Ref. [15] for a more extensive treatment).

4 Synchronization of n Different Gyros

Consider n different, independent gyros described by the nonautonomous nonlinear equations,

$$\ddot{\theta}_i = -\alpha_i^2\frac{(1-\cos\theta_i)^2}{\sin^3\theta_i} - c_i\dot{\theta}_i - e_i\dot{\theta}_i^3 + \beta_i \sin\theta_i - (\gamma_i \sin\theta_i)\sin\omega_i t \quad i = 1,2,\ldots,n \tag{12a}$$

$$:= f_i(\theta_i,\dot{\theta}_i,t;P_i) \quad i = 1,2,\ldots,n \tag{12b}$$

with

$$\theta_i(t=0) = \theta_i^0 \text{ and } \dot{\theta}_i(t=0) = \dot{\theta}_i^0 \quad i = 1,2,\ldots,n \tag{13}$$

We have explicitly included the parameter set $P_i = \{\alpha_i,\beta_i,c_i,e_i,\gamma_i,\omega_i\}$ on the right hand side of Eq. (12*b*), indicating that each of the n symmetric gyros could have different physical characteristics and may be mounted on surfaces that harmonically vibrate vertically at different frequencies and with different amplitudes of vibration.

Our aim is to synchronize the motion of all n gyros so that $n-1$ of them "follow" the motion of the master gyro. Without any loss of generality, from here on we shall take the master gyro to be the first gyro in our set of n gyros and refer to it (the master gyro) by the subscript 1. Hence, we require

$$\theta_i(t) = \theta_1(t) \quad i = 2,\ldots,n \tag{14}$$

where $\theta_1(t)$ is the solution of the nonlinear, nonautonomous differential equation given in Eq. (12*a*) with $i=1$. We note that the equation set (Eq. (14)) constitutes a set of $n-1$ independent conditions. The problem of synchronization can be interpreted as one of ensuring that the tracking conditions (Eq. (14)) are satisfied by the gyros whose equations of motion are given by Eqs. (12*a*) and (12*b*). Alternatively, we think of this problem as one in which Eqs. (12*a*), (12*b*), and (13) represent an unconstrained, n degree of freedom, mechanical system on which the $n-1$ independent constraints (14) are required to be imposed. In fact, we can modify this set of constraints to include all the $s := n(n-1)/2$ constraints,

$$h_{ij}(t) = (\theta_i(t) - \theta_j(t)) = 0 \quad \forall\, i<j \quad i,j \in (1,n) \tag{15}$$

of which $(n-1)(n-2)/2$ are redundant, though all of them are consistent [11,16]. Enforcing these constraints would make the motion of all the gyros identical. As mentioned before, among these s constraints, only $(n-1)$ are independent. Noting that in general the initial conditions (Eq. (13)) may not satisfy the constraints (Eq. (14)) (or, alternatively, Eq. (15)), we further modify the constraints (Eq. (15)) to

$$\ddot{h}_{ij} + \delta\dot{h}_{ij} + kh_{ij} = 0 \quad \forall\, i<j \quad i,j \in (1,n) \tag{16}$$

where δ and k are positive constants [15]. Since the solution of the set of s equations given by Eq. (16) satisfies the condition that $h_{ij} \to 0$ as $t \to \infty$, we have asymptotic (and exponential) convergence toward the satisfaction of the constraints (Eq. (15)) and hence obtain synchronization of the n different gyros.

It is important to point out that by altering the parameters δ and k in Eq. (16), one can describe different "paths" taken by the system of gyros toward their eventual synchronization. For simplicity, we have chosen the same constants δ and k for each equation of the set (16). In general, we could have used different values of δ and k for the different equations in this set (provided all the equations in the set are consistent with one another), signifying our intent to synchronize some of the gyros earlier (in time) than others since the values of δ and k for each of the equations in the set (16) control the rate and nature of convergence of $h_{ij}(t)$ to zero. Even more generally than is shown in the Eq. (16), we could have chosen the paths toward synchronization to be described by any set of consistent second order nonlinear differential equations that would be globally asymptotic to the solution $h_{ij}=0$, $i<j$, $i,j \in (1,n)$, so that the paths taken by the different gyros toward synchronization can be controlled pretty much at will.

Equations (16) can be put in the form of Eq. (8) where the n vector $\mathbf{q}=[\theta_1,\theta_2,\ldots,\theta_n]^T$, so that

$$\mathbf{A}\ddot{\mathbf{q}} = -\delta\mathbf{A}\dot{\mathbf{q}} - k\mathbf{A}\mathbf{q} := \mathbf{b}(\mathbf{q},\dot{\mathbf{q}}) \tag{17}$$

where matrix $\mathbf{A}$ is an $s \times n$ matrix, containing 0's, 1's, and -1's. For example, when we have four gyros so $n=4$ and $s=6$, the 6×4 matrix $\mathbf{A}$ takes the form

$$\mathbf{A} = \begin{bmatrix} 1 & -1 & 0 & 0 \\ 1 & 0 & -1 & 0 \\ 1 & 0 & 0 & -1 \\ 0 & 1 & -1 & 0 \\ 0 & 1 & 0 & -1 \\ 0 & 0 & 1 & -1 \end{bmatrix} \tag{18}$$

We note the form of matrix **A**, which we will use to our advantage in our subsequent derivations: Each row of **A** has all its elements zero, except for two elements, which are 1 and −1. As expected, only $(n-1)$ rows of matrix **A** are linearly independent. Comparing Eq. (5) with Eq. (12*b*), we see that the matrix **M** that describes the unconstrained motion of the mechanical system consisting of n gyros is given by $\mathbf{M}=\mathbf{I}_n$. Also, the n components of the n vector **f** in Eq. (5) are given by the f_i's, $i=1,2,\ldots,n$ defined in Eq. (12*b*). From Eq. (10), the explicit generalized control force n vector, $\mathbf{F}^c$, required to enforce the constraint set (Eq. (17)) is given by

$$\mathbf{F}^c = \mathbf{A}^+(\mathbf{b} - \mathbf{A}\mathbf{f}) \tag{19}$$

where A^+ is the MP inverse of matrix **A**, the s vector **b** is given in Eq. (17), and the f_i given in Eq. (12*b*) form the n components of the n vector **f**. For $n=4$ and matrix **A** given in Eq. (18), we easily determine (this can be done using MATLAB or MAPLE)

$$\mathbf{A}^+ = \frac{1}{4}\begin{bmatrix} 1 & 1 & 1 & 0 & 0 & 0 \\ -1 & 0 & 0 & 1 & 1 & 0 \\ 0 & -1 & 0 & -1 & 0 & 1 \\ 0 & 0 & -1 & 0 & -1 & -1 \end{bmatrix} \tag{20}$$

which when substituted in relation (19) will yield the explicit control forces to exactly satisfy the s constraint equations (Eq. (17)) or, alternatively, (Eq. (16)).

Noting Eq. (9), we then see that the synchronized motion of the n gyros is obtained by providing the generalized control force f_i^c to the ith gyro, where f_i^c is the ith component of the n vector $\mathbf{F}^c$ obtained explicitly in Eq. (19). The equations of motion for the (asymptotically) synchronized gyros will then be

$$\ddot{\theta}_i = f_i(\theta_i, \dot{\theta}_i, t; P_i) + f_i^c \quad i = 1,2,\ldots,n \tag{21}$$

From Eq. (21), we observe that, in general, $f_1^c(t) \neq 0$. Hence, though the motion of all the gyros is fully synchronized (asymptotically) by subjecting the ith gyro to the control force f_i^c, the synchronized motion will, in general, not be that of the master gyro, unless $f_1^c=0$. In order to synchronize the motion of the $(n-1)$ slave gyros with the motion of the first (master, $i=1$) gyro, we then need to simply subtract the force f_1^c from each component of the control force n vector $\mathbf{F}^c$ determined from Eq. (19). (The proof of this statement is somewhat long, and in order not to disturb the flow of thought, we present it in Appendix B.) The active control force needed to be applied to synchronize the remaining $n-1$ gyros with the motion of the first (master) gyro is then given by

$$\mathbf{F}^{\text{syn}} = \mathbf{F}^c - [\mathbf{1}]f_1^c = [0, f_2^c - f_1^c, f_3^c - f_1^c, \ldots, f_n^c - f_1^c]^T \tag{22}$$

where $[\mathbf{1}]$ denotes the $n\times 1$ column vector each of whose elements is unity.

We thus obtain the equations of motion of the system of n gyros as

$$\ddot{\theta}_i = f_i(\theta_i, \dot{\theta}_i, t; P_i) + f_i^{\text{syn}} \quad i = 1,2,\ldots,n \tag{23}$$

where f_i^{syn} is the ith component of the control force n vector F^{syn} (explicitly given in Eq. (22)), which causes the slave gyros to exactly follow the motion of the master. Note that the first component of the n vector $\mathbf{F}^{\text{syn}}$ is zero since the first gyro ($i=1$) is the master gyro, so that from Eq. (23), we have $\ddot{\theta}_1 = f_1(\theta_1, \dot{\theta}_1, t; P_1)$. The nonidentical slave gyros $(i=2,3,\ldots,n)$ are subjected to the last $(n-1)$ components of the generalized control force n vector $\mathbf{F}^{\text{syn}}$, which thus enforces exact synchronization of the slave gyros with the master gyro's motion.

5 Numerical Examples

In this section, we consider two examples. The first example deals with the synchronization of three nonidentical gyros, each with its own physical characteristics. For the parameters chosen to describe these gyros, each gyro exhibits chaotic dynamics, and the two slave gyros are required to follow the master's chaotic motions. The second example deals with five different gyros, whose motion is required to be synchronized. One of the four slave gyros in this set has properties that show regular motion, the others have properties that show chaotic motions. They are synchronized with the motion of the master gyro, which in this example is periodic, though complex.

Example 1. Consider three gyros each described by Eqs. (12*a*) and (12*b*) that need to be synchronized so that they each follow the motion of the first (master) gyro. Each uncontrolled gyro exhibits a chaotic motion. We shall take these three dynamical systems to be different from each other, described by the parameter sets $P_i=\{\alpha_i,\beta_i,c_i,e_i,\gamma_i,\omega_i\}$, $i=1,2,3$, and their dynamics will be investigated for the initial condition sets $\text{IC}_i=\{\theta_i^0, \dot{\theta}_i^0\}$, $i=1,2,3$, given by

$$P_1 = \{10,1,0.5,0.03,35.8,2.05\} \quad \text{IC}_1 = \{\theta_1^0 = -0.5, \dot{\theta}_1^0 = 1\} \tag{24}$$

$$P_2 = \{10,1,0.5,0.05,35.5,2\} \quad \text{IC}_2 = \{\theta_2^0 = 0.5, \dot{\theta}_2^0 = 1\} \tag{25}$$

and

$$P_3 = \{10.5,1,0.5,0.04,38.5,2.1\} \quad \text{IC}_3 = \{\theta_3^0 = 1, \dot{\theta}_3^0 = -0.5\} \tag{26}$$

The equation of motion (Eq. (12*a*)) for the ith gyro can be expressed as a set of three first order autonomous equations given by

$$\dot{\theta}_i = \upsilon_i$$

$$\dot{\upsilon}_i = -\alpha_i^2 \frac{(1-\cos\theta_i)^2}{\sin^3\theta_i} - c_i\upsilon_i - e_i\upsilon_i^3 + \beta_i \sin\theta_i - (\gamma_i \sin\theta_i)\sin\tau_i$$

$$\dot{\tau}_i = \omega_i \tag{27}$$

Each of the gyro systems described by the parameter sets P_i, $i=1,2,3$, given by Eqs. (24)–(26) is chaotic and has a different chaotic attractor.

The Lyapunov exponents for each of the dynamical systems are computed over a time span of 1000 s using the method described in Ref. [17]. The integration for determining these exponents is performed using MATLAB ODE45 using a relative error tolerance of 10^{-9} and an absolute error tolerance of 10^{-13}. The Lyapunov exponent sets, l_i, of the three different dynamical systems are computed to be $l_1 \approx \{0.211, -0.896, 0\}$, $l_2 \approx \{0.216, -1.001, 0\}$, and $l_3 \approx \{0.208, -0.936, 0\}$. The positive value of the largest Lyapunov exponent in each set indicates that the motions are chaotic for each of these gyros. Furthermore, the chaotic attractors for each system are different.

Figure 2 shows plots of $(\theta_i, \dot{\theta}_i)$, $i=1,2,3$, for $50 \leqslant t \leqslant 100$ for the three uncoupled gyros along with a figure (lower right corner) in which all three plots are superposed. The integration of the equations of motion throughout this study is carried out using MATLAB ODE45 with a relative error tolerance of 10^{-9} and an absolute error tolerance of 10^{-12}. The differences in the responses between the three gyros, $h_{ij}(t) = \theta_i(t) - \theta_j(t)$, are shown in Fig. 3.

We shall now use the scheme described in Sec. 4 to couple these gyros and synchronize them, the first gyro being the master. In this demonstration, the synchronization is done using equation

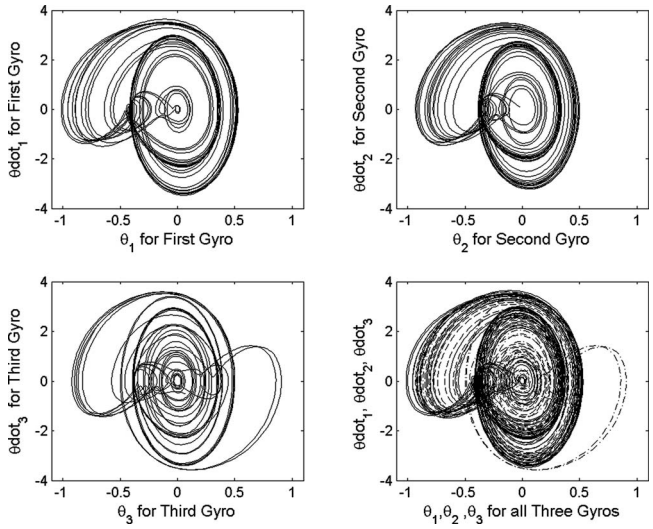

Fig. 2 $(\theta_i, \dot{\theta}_i)$ plots showing the dynamics of the three uncoupled gyros for $50 \leqslant t \leqslant 100$. The lower right corner shows these plots superposed on one another; the first gyro is shown with a solid line, the second with a dashed line, and the third with a dashed-dotted line.

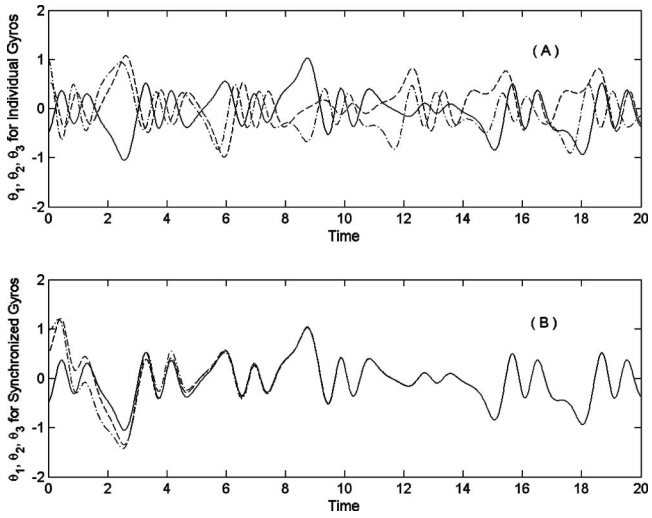

Fig. 4 (*A*) First 20 s of the response of the uncoupled gyros with the master gyro shown with a solid line, the second gyro shown with a dashed line, and the third gyro shown with a dashed-dotted line. (*B*) Synchronization of the gyros showing the slave gyros following the master (solid line), as required by the constraint set (16) with $\delta=1$ and $k=2$.

set (16) using $\delta=1$ and $k=2$. Since we have three dynamical systems, the number of constraints for synchronization are given by $s=3$. Matrix $\mathbf{A}$ becomes

$$\mathbf{A} = \begin{bmatrix} 1 & -1 & 0 \\ 1 & 0 & -1 \\ 0 & 1 & -1 \end{bmatrix} \tag{28}$$

so that

$$\mathbf{A}^{+} = \frac{1}{3}\begin{bmatrix} 1 & 1 & 0 \\ -1 & 0 & 1 \\ 0 & -1 & -1 \end{bmatrix} \tag{29}$$

We note that only two rows of matrix $\mathbf{A}$ given in relation (28) are independent, signifying that we have two constraints that are independent. The explicit, generalized control forces f_i^{syn} required to be applied to the slave gyros $(i=2,3)$ are obtained using relations (17)–(22). Figure 4(*a*) shows the time responses for the first 20 s. of the three uncoupled gyros, and Fig. 4(*b*) shows their synchronized response, where the latter two gyros $(i=2,3)$ are now slaved to the first gyro. We observe that the error between the responses gradually reduces to zero, as required by Eq. (17).

The plots in the $(\theta_i, \dot{\theta}_i)$ plane, $i=1,2,3$, superposed on one another for all three gyros are shown in Fig. 5, indicating synchronization of the two slave gyros with the chaotic motion of the master gyro. The plots are made using the response of each of the gyros over a 50 s interval of time starting at 50 s. We note that in this figure, there are three plots that are superimposed on top of one another.

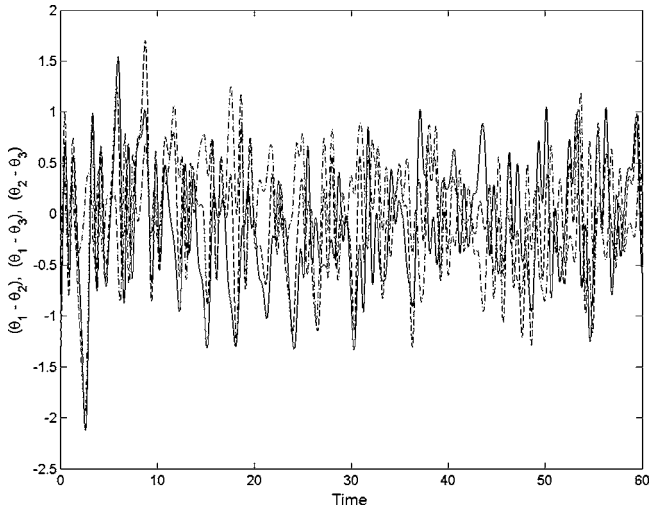

Fig. 3 The differences in the responses between the three uncoupled, unsynchronized gyros shown for a duration of 60 s. $h_{12}(t)=\theta_1(t)-\theta_2(t)$ is shown by the solid line, $h_{13}(t)=\theta_1(t)-\theta_3(t)$ is shown by the dashed line, and $h_{23}(t)=\theta_2(t)-\theta_3(t)$ is shown by the dashed-dotted line.

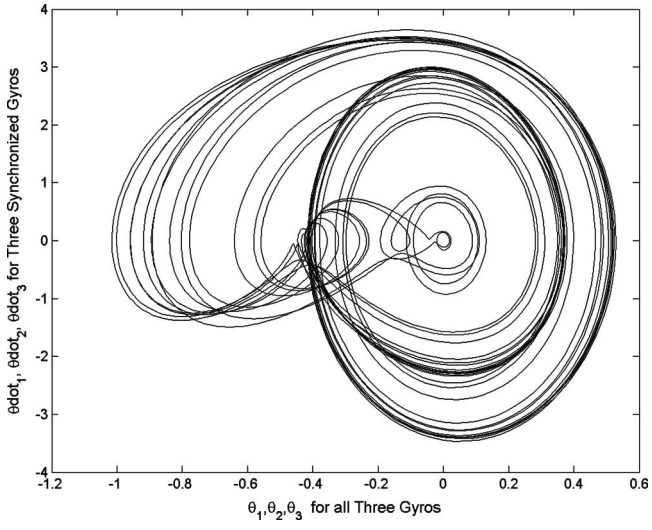

Fig. 5 Superimposed plots of $(\theta_i, \dot{\theta}_i)$, $i=1,2,3$, of the three synchronized gyros for $50 \leqslant t \leqslant 100$. The master gyro is a chaotic system and its Lyapunov exponents [17] are $l_1 \approx \{0.211, -0.896, 0\}$. Each of the gyros execute the entire motion shown in the plot.

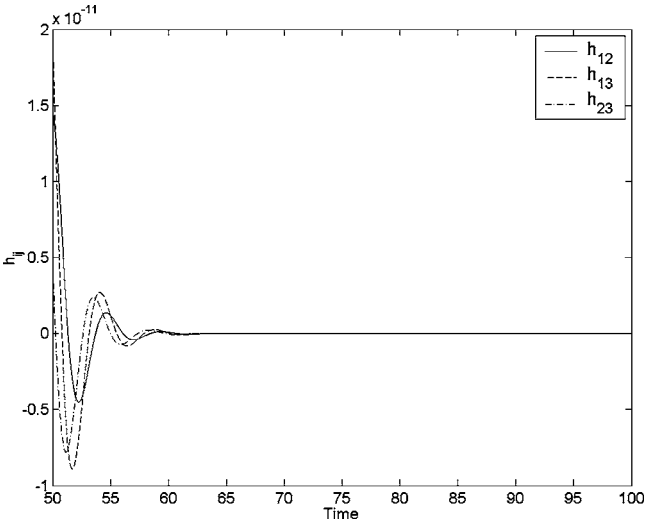

Fig. 6 $h_{12}(t)=\theta_1(t)-\theta_2(t)$ (solid line), $h_{13}(t)=\theta_1(t)-\theta_3(t)$ (dashed line), and $h_{23}(t)=\theta_2(t)-\theta_3(t)$ (dashed-dotted line) for $50\leqslant t\leqslant 100$. Note the exponential convergence of the h_{ij}'s, as demanded by Eq. (16), and also the vertical scale, which indicates that the error in synchronization is of the order of the numerical integration error tolerance, 10^{-12}.

The differences in the responses, $h_{ij}(t)=\theta_i(t)-\theta_j(t)$, $50\leqslant t\leqslant 100$, between the motions of the three synchronized gyros are shown in Fig. 6. We notice that this error soon becomes of the same order of magnitude as the numerical integration error tolerance (10^{-12}). The exponential convergence of $h_{ij}(t)$ toward zero, as demanded by relation (16), is obvious. Lastly, we show the generalized control forces that need to be applied to the slave gyros ($i=2,3$) to synchronize their motions with that of the master. This is shown in Fig. 7 for the entire time segment $0\leqslant t\leqslant 100$.

Example 2. We consider here five different gyro systems, and our aim is to track the motion of the first gyro (master, with parameter set P_1), which in this case is a periodic motion, though considerably complex in nature (see Fig. 9). The four slave gyros exhibit both regular and chaotic motions when uncontrolled. The

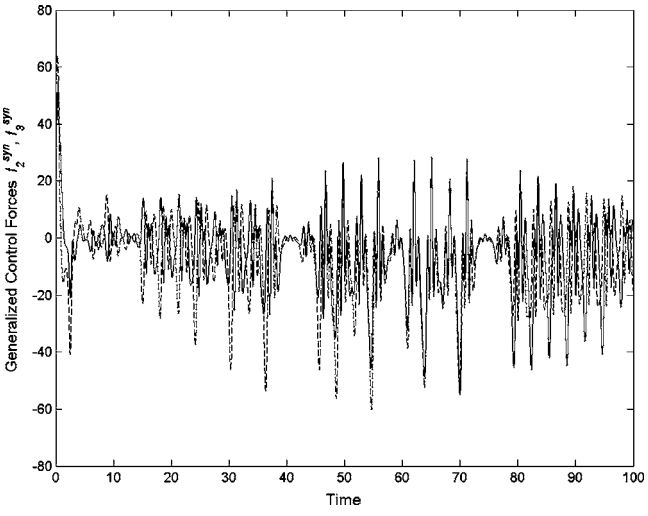

Fig. 7 The solid line shows the generalized force f_2^{syn} required to be applied to second gyro ($i=2$) to achieve synchronization with the motion of the master gyro ($i=1$). The dashed line shows the generalized force f_3^{syn} required to be applied to the third gyro ($i=3$).

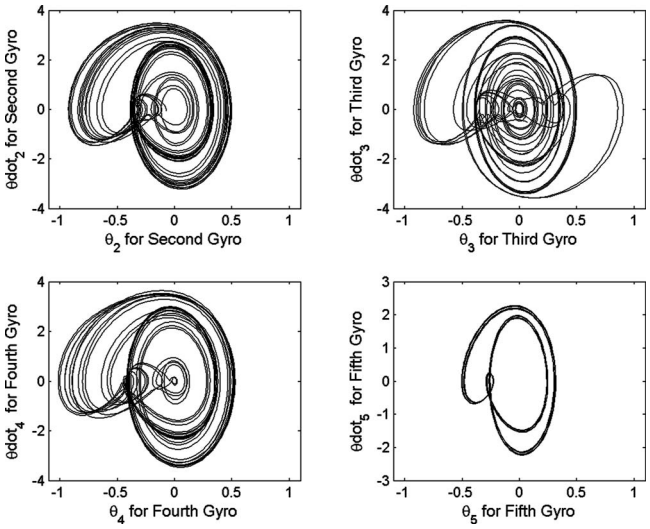

Fig. 8 $(\theta_i,\dot{\theta}_i)$, $i=2,3,4,5$ plot for $50\leqslant t\leqslant 100$ of the four uncoupled slave gyro systems showing different dynamical behaviors for each gyro. The lower right figure shows the transient motions of this ($i=5$) dynamical system, which has not yet attained its regular periodic behavior. The other three dynamical systems ($i=2,3,4$) exhibit chaotic motions, as indicated by the computed Lyapunov exponents.

parameter sets $P_i=\{\alpha_i,\beta_i,c_i,e_i,\gamma_i,\omega_i\}$, $i=1,2,\ldots,5$, and the initial condition sets for the dynamical systems are taken to be

$$P_1=\{10.5,1,0.5,0.02,38.7,2.2\}\quad \mathrm{IC}_1=\{\theta_1^0=-1,\dot{\theta}_1^0=0.5\} \tag{30}$$

$$P_2=\{10,1,0.5,0.05,35.5,2\}\quad \mathrm{IC}_2=\{\theta_2^0=0.5,\dot{\theta}_2^0=1\} \tag{31}$$

$$P_3=\{10.5,1,0.5,0.04,38.5,2.1\}\quad \mathrm{IC}_3=\{\theta_3^0=1,\dot{\theta}_3^0=-0.5\} \tag{32}$$

$$P_4=\{10,1,0.5,0.03,35.8,2.05\}\quad \mathrm{IC}_4=\{\theta_4^0=-0.5,\dot{\theta}_4^0=1\} \tag{33}$$

and

$$P_5=\{10.5,1,0.45,0.045,36,2.05\}\quad \mathrm{IC}_5=\{\theta_5^0=0.5,\dot{\theta}_5^0=0.5\} \tag{34}$$

The Lyapunov exponent sets, l_i, for these five different gyros—three of which have the same properties as those in Example 1—computed over a time interval of 1000 s, are found to be [17]

$$l_1\approx\{-0.180,-0.50,0\}\quad l_2\approx\{0.216,-1.001,0\}$$
$$l_3\approx\{0.208,-0.936,0\}$$
$$l_4\approx\{0.211,-0.896,0\}\quad l_5\approx\{-0.017,-0.606,0\} \tag{35}$$

The numerical integration error tolerances for computing the Lyapunov exponents are identical to those used in the previous example. From the values of set l_1, we see that the master gyro has a periodic motion, while the slave gyros ($i=2,3,4,5$) show a variety of both chaotic and regular motions. From the largest Lyapunov exponent, we see that three of the slaves exhibit chaotic motions, while one shows a periodic motion.

Figure 8 shows the $(\theta_i,\dot{\theta}_i)$, $i=2,3,4,5$ plots for the four slave gyro systems for $50\leqslant t\leqslant 100$. Except for the dynamical system

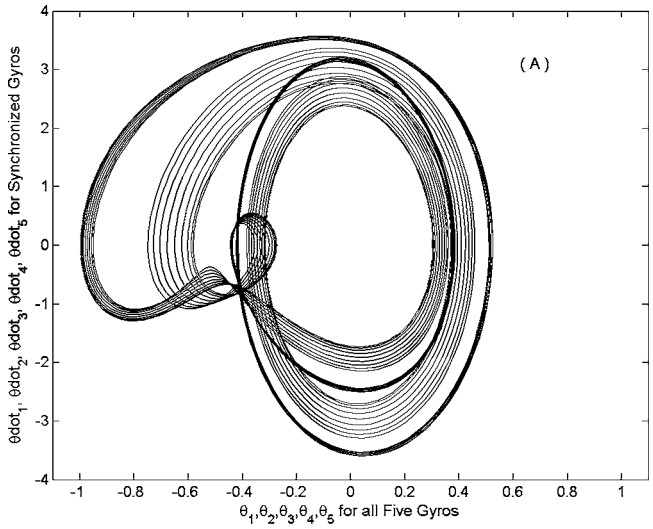

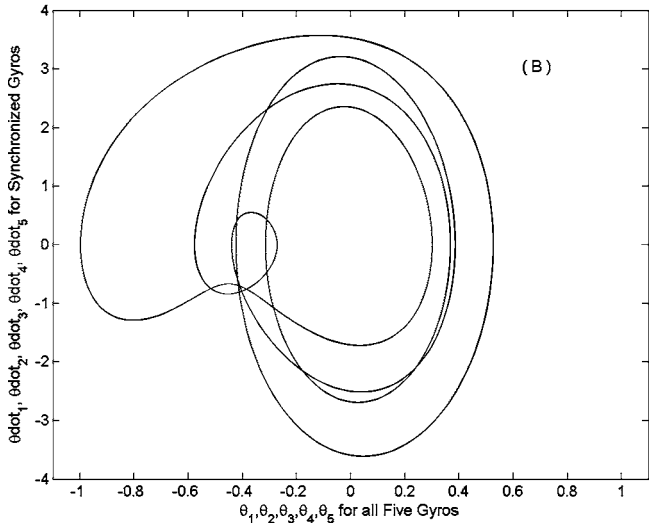

Fig. 9 (*A*) $(\theta_i, \dot{\theta}_i)$, $i=1,2,3,4,5$, plot for $50 \leq t \leq 100$ of the five gyro systems superimposed on each other showing that the four slaves follow the master gyro. As is seen, the motion of the master is a complex transient motion, which has not yet reached its stable periodic orbit, which is characterized by the Lyapunov exponents $l_1 \approx \{-0.180, -0.50, 0\}$. (*B*) $(\theta_i, \dot{\theta}_i)$, $i=1,2,3,4,5$, plot for $150 \leq t \leq 200$ of the five gyro systems superimposed on each other showing that the four slaves follow the master gyro. The master gyro has reached a periodic orbit, and the four slaves synchronize with the master's motion. The motion of the five gyros is shown superposed on each other.

$(i=5)$ shown in the lower right, the other three slaves exhibit a chaotic behavior, as indicated from the computed Lyapunov numbers shown in Eq. (35).

The synchronized motion—we again choose $\delta=1$ and $k=2$—of the five systems with the four slaves following the master is shown in Fig. 9(*a*). We see that the tracking during the transient period when the orbit of the master gyro is being attracted to its stable periodic orbit is very well executed by the control. Here, the uncontrolled motion of the first (master) gyro is first plotted, and superimposed on it are plots of the motions of the four slaves for $50 \leq t \leq 100$. The results of the synchronization procedure when the integration is extended to 200 s are shown in Fig. 9(*b*), where we have plotted the motions of the five different systems for $150 \leq t \leq 200$. The plots fall exactly on top of each other, indicating synchronization. We notice that the master gyro's motion has now settled down to being periodic, and the four slaves follow this periodic, though complex, motion. Note that the figure shows the motion of all five gyros superposed on one another.

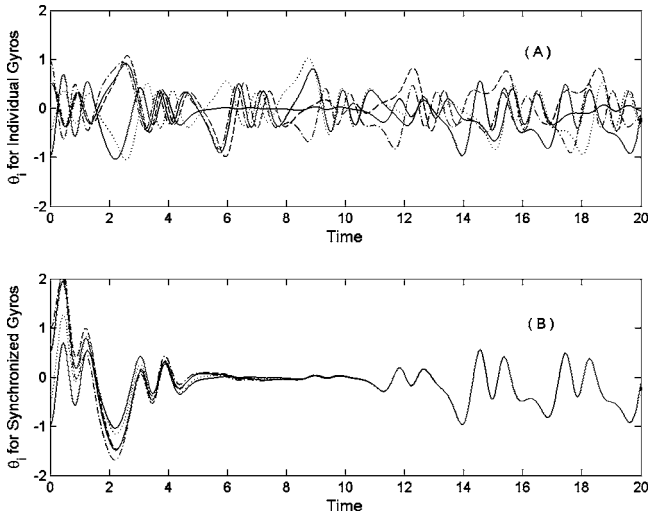

Fig. 10 The upper figure shows the motion of the five uncoupled gyros over the first 20 s. of response. The lower figure shows the manner in which the synchronization occurs over time, the five gyros following the motions of the master gyro, which in turn is asymptotically attracted to a stable periodic orbit, as shown in Fig. 9(*b*).

The manner in which the synchronization occurs over time is illustrated in Fig. 10, where we show the first 20 s. of the motion of both the uncoupled system and the synchronized system. The solid line in the two panels denotes the master gyro; the dashed line, the second gyro; the dashed-dotted line the third gyro; the dotted line, the fourth gyro; and another solid line, the fifth. From the lower panel, which shows synchronization with the master gyro, we can identify the motion of the master in the upper panel.

Figure 11 shows the control forces needed to be applied to the four slave gyros for synchronization for $0 \leq t \leq 100$. The errors in synchronization, $h_{ij}(t)=\theta_i(t)-\theta_j(t)$, for the time intervals $50 \leq t$

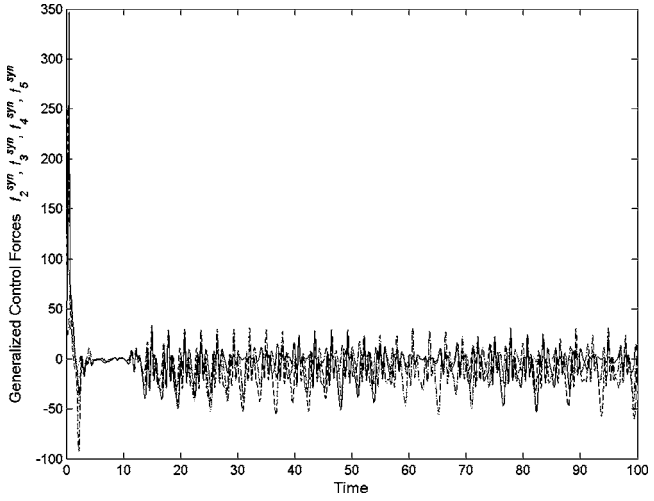

Fig. 11 Control forces required to be applied to the four slave gyros. The solid line shows the generalized control force on the second gyro, the dashed line that on the third gyro, the dashed-dotted line that on the fourth gyro, and the dotted line that on the fifth gyro.

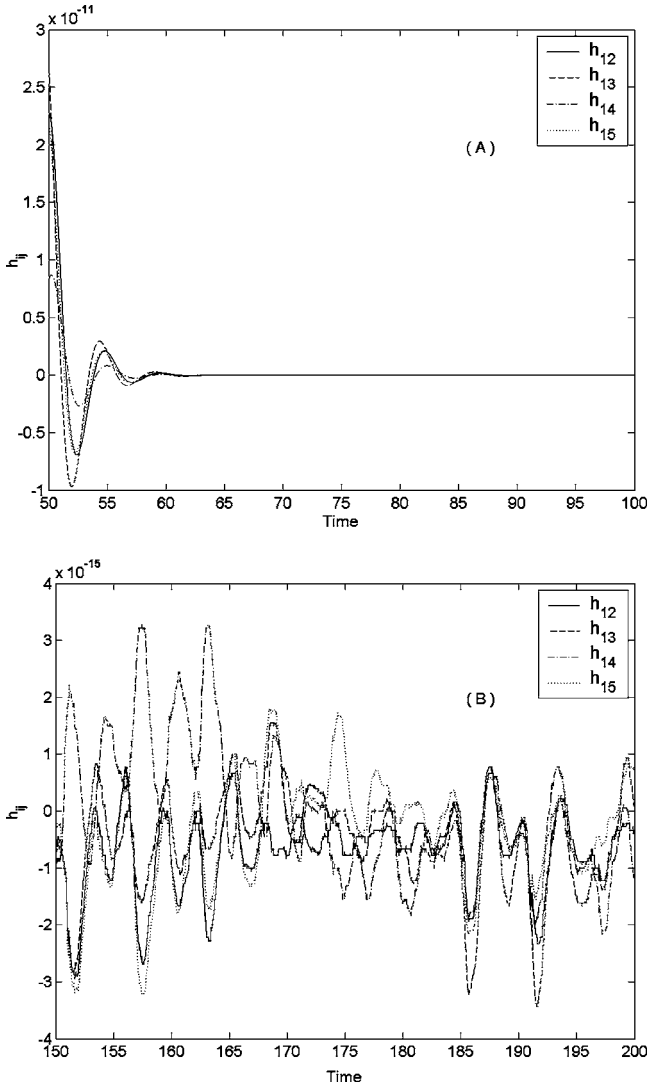

Fig. 12 (*A*) The errors $h_{ij}(t)$ as functions of time for $50 \leqslant t \leqslant 100$, showing that they exponentially reduce. (*B*) The errors $h_{ij}(t)$ as functions of time for $150 \leqslant t \leqslant 200$. Note the vertical scales. Errors in synchronization of the motion are less than the integration error tolerance used.

$\leqslant 100$ and $150 \leqslant t \leqslant 200$ are shown in Fig. 12, which shows the same sort of characteristics, including exponential convergence, that were observed earlier in Fig. 6.

6 Conclusions

In this paper, we have described an analytical dynamics based approach to the synchronization of highly nonlinear mechanical systems that yields the explicit generalized active control forces so that a set of slave systems can follow an independent master mechanical system. This paper focuses on gyroscopic systems—by way of demonstration—due to their importance in the guidance and control of airships and spacecraft and in the accurate control of complex mechanical systems, such as robotic and autonomous systems. While for simplicity, the slave systems have been considered to be independent of each other in this paper, the same methodology is applicable to slave systems that may be linearly or nonlinearly coupled to one another. The main contributions of this paper are the following.

1 The novel strategy used here is to formulate the problem of synchronization of highly nonlinear mechanical systems first as a tracking control problem, and then further recast this tracking control problem as a problem of constrained motion of nonlinear dynamical systems. We accordingly constrain the motion of the slave systems to exactly follow the master system and thereby obtain the exact control forces required to be applied to the slaves for synchronization with the master. The constraint (control) forces that need to be applied for exact synchronization are determined *explicitly* and in *closed form* using the newly developed general theory of constrained motion of nonlinear mechanical systems. The theory [11,15] that underlies the approach is much broader than what is required for the specific problem at hand of synchronizing chaotic/regular gyroscopic systems since it is applicable to general nonlinear mechanical systems. This makes the approach presented here applicable to the synchronization of general nonlinear systems.
2 In Sec. 4 and Appendix B, we prove a general result that hereto appears to be not known, and we use it to develop a simple, yet powerful, methodology for the synchronization of complex nonlinear mechanical systems.
3 The method yields control forces for the synchronization of nonlinear mechanical systems that have the following salient and beneficial characteristics. The control forces (1) are continuous in time, (2) are obtained explicitly in closed form so that they are simple and efficacious to determine, (3) lead, theoretically speaking, to exact synchronization of the nonlinear mechanical systems, (4) provide, in a sense, the *minimum forces* that need to be exerted for such synchronization [18], and (5) are not found by methods using any approximations of the nonlinear system.
4 Whereas most such synchronization studies are done with dynamical systems that are identical, we show that the method developed here can be used with equal ease and facility to couple *different* slave systems—each displaying varying kinds of regular and chaotic motions. This is important because, unlike many electrical systems, multiple copies of mechanical systems can seldom be built to have identical dynamical characteristics.
5 We show the efficacy of the methodology by illustrating two examples. In the first example, two slave gyros with different dynamical characteristics are synchronized with the motions of yet another master gyro whose dynamical characteristics differ from those of both the slaves; the master's motion is chaotic. In the second example, we consider five different gyro systems, some of which have chaotic motions, and we synchronize them with the stable periodic motions of the master gyro. While the dynamics of the slave gyros have been taken for simplicity to be independent of one another in this paper, the same general methodology works with coupled slave gyros as well.
6 We observe that while most methods (e.g., Ref. [10]) of synchronization deal with applying control signals to each of the first order differential equations that describe a mechanical system's dynamics (each gyro here can be represented by three, first order autonomous, nonlinear equations), the method proposed here deals directly, and simply, with the second order nonautonomous Lagrange equations of motion and obtains in explicit form the generalized control forces required to synchronize the different mechanical systems. The control we obtain is continuous in time, unlike what might be obtained using methods such as sliding mode control [20]; yet, theoretically speaking, it leads to exact synchronization.
7 Lastly, the approach allows the paths in phase space along which the synchronization occurs to be easily and accurately controlled, so that different slaves can be brought into synchronization with the master with varying levels of rapidity, as desired.

Appendix A

The Lagrangian in Eq. (1) can be obtained as follows:

1 The kinetic energy (KE) of the symmetrical gyro (Fig. 1) with respect to the inertial frame of reference $OXYZ = (1/2)m\bar{u}_{\text{c.m.}} \cdot \bar{u}_{\text{c.m.}} + \text{KE}$ of rotation about the c.m. of the gyro. Here, $\bar{u}_{\text{c.m.}}$ is the velocity of the c.m. of the gyro with respect to the inertial frame $OXYZ$. Denoting by $\bar{\mathbf{x}}_{\text{c.m.}}$ the position vector of the c.m. of the gyro, we have

$$\bar{x}_{\text{c.m.}} = (r \sin\varphi \sin\theta)\bar{\mathbf{I}} - (r \sin\theta \cos\varphi)\bar{\mathbf{J}} + (r \cos\theta + d)\bar{\mathbf{K}} \tag{A1}$$

where $\bar{\mathbf{I}}$, $\bar{\mathbf{J}}$, and $\bar{\mathbf{K}}$ are the unit vectors along the inertial coordinate directions OX, OY, and OZ, respectively. Differentiating Eq. (A1) with respect to time and noting that the vertical support excitation $d(t) = d_0 \sin \omega t$, we obtain the velocity of the c.m. of the gyro to be

$$\bar{u}_{\text{c.m.}} = (r\dot{\theta} \sin\varphi \cos\theta + r\dot{\varphi} \cos\varphi \sin\theta)\bar{\mathbf{I}} + (r\dot{\varphi} \sin\varphi \sin\theta - r\dot{\theta} \cos\varphi \cos\theta)\bar{\mathbf{J}} + (\dot{d} - r\dot{\theta} \sin\theta)\bar{\mathbf{K}} \tag{A2}$$

$$\text{Hence, } \bar{u}_{\text{c.m.}} \cdot \bar{u}_{\text{c.m.}} = r^2(\dot{\theta}^2 + \dot{\varphi}^2 \sin^2\theta) + \dot{d}^2 - 2r\dot{d}\dot{\theta} \sin\theta \tag{A3}$$

The total KE of the gyro [14] is then given by

$$\text{KE} = \frac{1}{2}m[r^2(\dot{\theta}^2 + \dot{\varphi}^2 \sin^2\theta) + \dot{d}^2 - 2r\dot{d}\dot{\theta} \sin\theta] + \frac{1}{2}I_1(\dot{\theta}^2 + \dot{\varphi}^2 \sin^2\theta) + \frac{1}{2}I_3(\dot{\psi} + \dot{\varphi} \cos\theta)^2 \tag{A4}$$

Here, I_1 and I_3 refer to the moments of inertia about the equatorial and polar directions through the c.m. of the symmetric gyro. This expression simplifies to

$$\text{KE} = \frac{1}{2}I(\dot{\theta}^2 + \dot{\varphi}^2 \sin^2\theta) + \frac{1}{2}I_3(\dot{\psi} + \dot{\varphi} \cos\theta)^2 - mr\dot{d}\dot{\theta} \sin\theta + \frac{1}{2}m\dot{d}^2 \tag{A5}$$

where $I = (mr^2 + I_1)$ is the moment of inertia of the gyro about an axis through the point of support o, which is parallel to the principal axis direction that goes through the c.m.

2 The potential energy (PE) of the gyro with respect to the inertial frame $OXYZ$ is

$$\text{PE} = mgd + mgr \cos\theta \tag{A6}$$

3 Therefore, the effective Lagrangian—we ignore terms that are purely functions of time—$L = \text{KE} - \text{PE}$, is then

$$L = \frac{1}{2}I(\dot{\theta}^2 + \dot{\varphi}^2 \sin^2\theta) + \frac{1}{2}I_3(\dot{\psi} + \dot{\varphi} \cos\theta)^2 - mr\dot{d}\dot{\theta} \sin\theta - mgr \cos\theta \tag{A7}$$

Appendix B

We obtain here the explicit control force n vector $\mathbf{F}^{\text{syn}}$, as given in Eq. (22), which is required to be applied to the set of n nonlinear mechanical systems so that the slave systems, $i = 2, 3, \ldots, n$, follow the master system, $i = 1$.

We begin with two lemmas.

LEMMA 1. *Consider the $s \times n$ matrix $\mathbf{A}$ of Eq. (17), an instantiation of which is provided for $n = 4$ in Eq. (18). Augment matrix $\mathbf{A}$ by the n-component row vector*

$$\mathbf{g} = [1, 0, 0, \ldots, 0] \tag{B1}$$

to form the $(s+1) \times n$ matrix

$$\tilde{\mathbf{A}} = \begin{bmatrix} \mathbf{A} \\ \mathbf{g} \end{bmatrix} \tag{B2}$$

Then, the row vector

$$\mathbf{h} := \mathbf{g}[\mathbf{I}_n - \mathbf{A}^+\mathbf{A}] \tag{B3}$$

is simply the n-component row vector $(1/n)[1, 1, \ldots, 1]$. Here, $\mathbf{X}^+$ denotes the MP inverse of the matrix $\mathbf{X}$.

Proof. We notice that only $(n-1)$ rows of matrix $\mathbf{A}$ are linearly independent. Hence, $\mathbf{A}$ is rank deficient. As shown in Ref. [13], the column space of the $n \times n$ matrix $[\mathbf{I}_n - \mathbf{A}^+\mathbf{A}]$ is the same as the null space of matrix $\mathbf{A}$. However, the null space of matrix $\mathbf{A}$ has dimension 1 and consists of n-component column vectors, each of the form $\lambda[1, 1, 1, \ldots, 1]^T$, where we disallow the value $\lambda = 0$ since it leads to a trivial vector. Thus, the n columns of the $n \times n$ matrix $[\mathbf{I}_n - \mathbf{A}^+\mathbf{A}]$ must be of the form $\lambda_i[1, 1, 1, \ldots, 1]^T$, $i = 1, 2, \ldots, n$, where the constants $\lambda_i \neq 0$, $i = 1, 2, 3, \ldots, n$, remain yet to be determined.

However, the matrix $[\mathbf{I}_n - \mathbf{A}^+\mathbf{A}]$ is symmetric since $[\mathbf{I}_n - \mathbf{A}^+\mathbf{A}]^T = \mathbf{I}_n - (\mathbf{A}^+\mathbf{A})^T = \mathbf{I}_n - (\mathbf{A}^+\mathbf{A})$ (see Ref. [13]). Hence, $\lambda_1 = \lambda_2 = \cdots = \lambda_n = \lambda$. Furthermore, $[\mathbf{I}_n - \mathbf{A}^+\mathbf{A}]$ is idempotent; hence, $n\lambda^2 = \lambda$, which implies that $\lambda = 1/n$. The matrix $[\mathbf{I}_n - \mathbf{A}^+\mathbf{A}]$ therefore has identical columns, and every entry in the matrix is $1/n$. Noting Eq. (B1), the result now follows.

From this proof, it follows that the result of this lemma is true even when our matrix $\mathbf{A}$ has any row dimension r, $(n-1) \leqslant r \leqslant s = n(n-1)/2$, provided it always has $(n-1)$ linearly independent rows. □

LEMMA 2. *The MP generalized inverse of matrix $\tilde{\mathbf{A}}$ defined in Eq. (B2) is given by*

$$\tilde{\mathbf{A}}^+ = [\mathbf{V}\mathbf{A}^+ \quad |[\mathbf{1}]] \tag{B4}$$

where $[1]$ is the n-component column vector each of whose components is unity, and the $n \times n$ matrix

$$\mathbf{V} = \left[\begin{array}{c|ccccc} 0 & 0 & \cdots & \cdots & \cdots & 0 \\ \hline -1 & & & & & \\ -1 & & & & & \\ \vdots & & & \mathbf{I}_{n-1} & & \\ \vdots & & & & & \\ -1 & & & & & \end{array}\right] \tag{B5}$$

where $\mathbf{I}_{n-1}$ is the $(n-1) \times (n-1)$ identity matrix.

Proof. Greville [19] gives the MP inverse of a matrix $\tilde{\mathbf{A}}$, which is obtained by augmenting any matrix $\mathbf{A}$ with the row $\mathbf{g}$, as

$$\tilde{\mathbf{A}}^+ = \begin{bmatrix} \mathbf{A} \\ \mathbf{g} \end{bmatrix}^+ = [(\mathbf{I}_n - \mathbf{h}^+\mathbf{g})\mathbf{A}^+ \quad |\mathbf{h}^+] \quad \text{for } \mathbf{h} = \mathbf{g}(\mathbf{I}_n - \mathbf{A}^+\mathbf{A}) \neq 0 \tag{B6}$$

For our specific matrix $\mathbf{A}$ and row vector $\mathbf{g}$, the row vector $\mathbf{h}$ is given by Eq. (B3). The MP inverse of $\mathbf{h}$, namely, $\mathbf{h}^+ = [1, 1, \ldots, 1]^T := [\mathbf{1}]$ (see Ref. [13]). Noting that $\mathbf{g} = [1, 0, 0, \ldots, 0]$, we have $(\mathbf{I}_n - \mathbf{h}^+\mathbf{g}) = V$, and the result follows equation (B6). □

Main Result

The control force that synchronizes the $(n-1)$ slave gyro systems to the motion of the first (master, $i = 1$) gyro is given by the n vector

$$\mathbf{F}^{\text{syn}} = \mathbf{F}^c - [\mathbf{1}]f_1^c = [0, f_2^c - f_1^c, f_3^c - f_1^c, \ldots, f_n^c - f_1^c]^T \tag{B7}$$

where the f_i^c's are defined as in Eqs. (19) and (21).

Proof. We add to the s constraints given by Eq. (17) the addi-

tional constraint $\ddot{q}_1 := \ddot{\theta}_1 = f_1(\theta_1, \dot{\theta}_1, t) = f_1(q_1, \dot{q}_1, t)$, so that our set of constraints now becomes

$$\tilde{\mathbf{A}}\ddot{\mathbf{q}} = \begin{bmatrix} \mathbf{A} \\ \mathbf{g} \end{bmatrix} \ddot{\mathbf{q}} = \begin{bmatrix} \mathbf{b}(\mathbf{q}, \dot{\mathbf{q}}) \\ f_1(q_1, \dot{q}_1, t) \end{bmatrix} := \tilde{\mathbf{b}}(\mathbf{q}, \dot{\mathbf{q}}, t) \tag{B8}$$

instead, where the column vector $\mathbf{b}$ is the same as that in Eq. (17), $\mathbf{g}$ is the row vector defined in Eq. (B1), and $\tilde{\mathbf{A}}$ is now an $(s+1) \times n$ matrix. The last constraint simply enforces the condition that the motion of the master gyro is not to be disturbed through the addition of any control force applied to it.

The control force that causes these constraints (Eq. (B8)) to be satisfied is then simply given, like before, by [13]

$$\mathbf{F}^{\text{syn}} = \tilde{\mathbf{A}}^{+}(\tilde{\mathbf{b}} - \tilde{\mathbf{A}}\mathbf{f}) \tag{B9}$$

where $\mathbf{f} = [f_1, f_2, \ldots, f_n]^T$. Using Lemma 2 and Eq. (B8), this can be rewritten as

$$\begin{aligned} \mathbf{F}^{\text{syn}} &= \tilde{\mathbf{A}}^{+}\left\{ \begin{bmatrix} \mathbf{b}(\mathbf{q}, \dot{\mathbf{q}}) \\ f_1(q_1, \dot{q}_1, t) \end{bmatrix} - \begin{bmatrix} \mathbf{A} \\ \mathbf{g} \end{bmatrix} \mathbf{f} \right\} \\ &= \tilde{\mathbf{A}}^{+} \begin{bmatrix} \mathbf{b} - \mathbf{A}\mathbf{f} \\ 0 \end{bmatrix} = [\mathbf{V}\mathbf{A}^{+} \quad |[\mathbf{1}]] \begin{bmatrix} \mathbf{b} - \mathbf{A}\mathbf{f} \\ 0 \end{bmatrix} \end{aligned} \tag{B10}$$

where matrix $\mathbf{V}$ is defined in Eq. (B5).

Since $\mathbf{F}^c := [f_1^c, f_2^c, f_3^c, \ldots, f_n^c]^T = \mathbf{A}^{+}(\mathbf{b} - \mathbf{A}\mathbf{f})$, as given in Eq. (19), relation (B10) becomes

$$\mathbf{F}^{\text{syn}} = [\mathbf{V}\mathbf{A}^{+} \quad |[\mathbf{1}]] \begin{bmatrix} \mathbf{b} - \mathbf{A}\mathbf{f} \\ 0 \end{bmatrix} = \mathbf{V}\mathbf{F}^c \tag{B11}$$

Noting the form of $\mathbf{V}$ in Lemma 2, equation (B11) thus reduces to

$$\mathbf{F}^{\text{syn}} = \mathbf{V}\mathbf{F}^c = [0, f_2^c - f_1^c, f_3^c - f_1^c, \ldots, f_n^c - f_1^c]^T \tag{B12}$$

which is the required result. As expected, there is no control force required to be applied to the master gyro because this is the motion that we are requiring the slave gyros to follow.

It is important to note that from all the control forces $\hat{\mathbf{F}}^{\text{syn}}(t)$ that can be applied to the system to cause synchronization, the control force $\mathbf{F}^{\text{syn}}(t)$, which is given explicitly in equation (B12), minimizes at each instant of time the quantity $[\hat{\mathbf{F}}^{\text{syn}}(t)]^T \hat{\mathbf{F}}^{\text{syn}}(t)$ (see Ref. [18]). That is, of all the control forces that will cause synchronization, $F^{\text{syn}}(t)$ has, *at each instant of time*, the smallest Euclidean norm. □

COROLLARY. The result above is valid when we use *any* r appropriate and consistent equations, $(n-1) \leqslant r \leqslant s = n(n-1)/2$ for synchronization, of the form

$$\theta_i(t) = \theta_j(t) \quad i < j \quad i, j \in (1, n) \tag{B13}$$

to synchronize the $(n-1)$ nonlinear mechanical systems with the master system $(i=1)$, as long as $(n-1)$ of these equations are linearly independent.

Proof. If the conditions of the corollary are satisfied, the rank of the $r \times n$ matrix $\mathbf{A}$ is $(n-1)$, and the null space of $\mathbf{A}$ will have dimension 1. Noting the form of $\mathbf{A}$, the columns of the $n \times n$ matrix $[\mathbf{I}_n - \mathbf{A}^{+}\mathbf{A}]$ will then each be of the form $\lambda[1, 1, \ldots, 1]^T$. According to Lemma 1 then,

$$\mathbf{h} := \mathbf{g}[\mathbf{I}_n - \mathbf{A}^{+}\mathbf{A}] = (1/n)[1, 1, \ldots, 1] \tag{B14}$$

so that, again,

$$\mathbf{h}^{+} = [1, 1, \ldots, 1]^T := [\mathbf{1}] \tag{B15}$$

and the entire argument goes through. □

References

[1] Tong, X., and Mrad, N., 2001, "Chaotic Motion of a Symmetric Gyro Subjected to Harmonic Base Excitation," ASME J. Appl. Mech., **68**, pp. 681–684.

[2] Ge, Z.-M., and Chen, H.-H., 1996, "Bifurcation and Chaos in Rate Gyro With Harmonic Excitation," J. Sound Vib., **194**(1), pp. 107–117.

[3] Ge, Z.-M., Chen, H.-K., and Chen, H.-H., 1996, "The Regular and Chaotic Motions of a Symmetric Heavy Gyroscope With Harmonic Excitation," J. Sound Vib., **198**(2), pp. 131–147.

[4] Chen, H.-K., 2002, "Chaos and Chaos Synchronization of a Symmetric Gyro With Linear-Plus-Cubic Damping," J. Sound Vib., **255**(4), pp. 719–740.

[5] Van Dooren, R., 2003, "Comments on Chaos and Chaos Synchronization of a Symmetric Gyro With Linear-Plus-Cubic Damping," J. Sound Vib., **268**, pp. 632–634.

[6] Leipnik, R. B., and Newton, T. A., 1981, "Double Strange Attractors in Rigid Body Motion With Linear Feedback Control," Phys. Lett., **86A**, pp. 63–67.

[7] Pecora, L.-M., and Carroll, T. L., 1990, "Synchronization in Chaotic Systems," Phys. Rev. Lett., **64**, pp. 821–824.

[8] Lakshmanan, M., and Murali, K., 1996, *Chaos in Nonlinear Oscillators: Controlling Synchronization*, World Scientific, Singapore.

[9] Strogatz, S., 2000, *Nonlinear Dynamics and Chaos*, Westview, Cambridge, MA.

[10] Lei, Y., Xu, W., and Zheng, H., 2005, "Synchronization of Two Chaotic Nonlinear Gyros Using Active Control," Phys. Lett. A, **343**, pp. 153–158.

[11] Udwadia, F. E., and Kalaba, R. E., 1996, "Analytical Dynamics: A New Approach," Cambridge University Press, Cambridge, England.

[12] Hramov, A., and Koronovskii, A., 2005, "Generalized Synchronization: A Modified System Approach," Phys. Rev. E, **71**(6), P. 067201.

[13] Boccaletti S., Kruths, J., Osipov, G., Valladares, D., and Zhou, C., 2002, "The Synchronization of Chaotic Systems," Phys. Rep., **336**, pp. 1–101.

[14] Pars, L. A., 1972, *A Treatise on Analytical Dynamics*, Oxbow, Woodbridge, CT.

[15] Udwadia, F. E., 2003, "A New Perspective on the Tracking Control of Nonlinear Structural and Mechanical Systems," Proc. R. Soc. London, Ser. A, **459**, pp. 1783–1800.

[16] Franklin, J., 1995, "Least-Squares Solution of Equations of Motion Under Inconsistent Constraints," Linear Algebr. Appl., **222**, pp. 9–13.

[17] Udwadia, F. E., and von Bremen, H., 2001, "An Efficient and Stable Approach for Computation of Lyapunov Characteristic Exponents of Continuous Dynamical Systems, Appl. Math. Comput., **121**, pp. 219–259.

[18] Udwadia, F. E., 2000, "Fundamental Principles of Lagrangian Dynamics: Mechanical Systems With Non-Ideal, Holonomic, and Non-Holonomic Constraints," J. Math. Anal. Appl., **252**, pp. 341–355.

[19] Udwadia, F. E., and Kalaba, R. E., 1997, "An Alternative Proof of the Greville Formula," J. Optim. Theory Appl., **94**(1), pp. 23–28.

[20] Utkin, V., 1992, *Sliding Modes in Control Optimization*, Springer-Verlag, Berlin.